JOURNAL OF AGRICULTURAL AND FOOD CHEMISTRY

Single-Sided and Semisingle-Sided NMR Sensors for Highly Diffusive Samples: Application to Bottled Beverages

HOLGER STORK, ACHIM GÄDKE, AND NIKOLAUS NESTLE*

Institute of Condensed Matter Physics, TU Darmstadt, Hochschulstrasse 6, D-64289 Darmstadt, Germany

Single-sided NMR sensors such as the NMR-MOUSE have been very successfully implemented for quality control applications in the rubber and polymer industries. More recently, single-sided NMR was also applied in characterization of the fat components in foods. Both industrial polymers and the fat components in food exhibit relatively low self-diffusion coefficients on the order of 5×10^{-11} m^2/s or lower. The application of conventional single-sided NMR to highly mobile, watery phases in foods and beverages is hampered by the strong magnetic field gradient present in standard single-sided NMR devices. In this contribution, we present both a single-sided NMR sensor with a reduced magnetic field gradient and another ("semisingle-sided") sensor design with an open sample bay using a single-sided RF coil. The latter design allows much better sensitivity without sacrificing the necessary open access needed for measurements on entire food packages such as bottles. As a first application, the sensors were used for determining the oxygen content in bottles with superoxygenated table water.

KEYWORDS: TD-NMR; relaxation; diffusion; single-sided NMR; beverages; oxygenated table water

INTRODUCTION

Low-field proton nuclear magnetic resonance (NMR) is a technique that is widely used in the food industry, with the main application being the determination of the solid/liquid ratio of fat blends (*1*, *2*). In contrast to high-field NMR, no spectral information can be obtained in low-field NMR. Rather, the behavior of the NMR response in the time domain is studied. For this reason, low-field NMR is often also known as time−domain NMR (TD-NMR). The information available from TD-NMR experiments includes proton spin relaxation times and—with slightly more sophisticated approaches—also diffusion coefficients. Traditionally, TD-NMR is carried out on small samples in test tubes with a diameter around 1 cm. These vials are put into the RF sample coil of the NMR setup, which is located inside a fairly homogeneous magnetic field (typically about 0.5 T). The sample size is dictated by the size of the air gap in the magnet system and the diameter of the sample coil. This kind of TD-NMR has been successfully applied to many areas of food science, e.g., dairy products (*3*), starch preparations (*4*), and bakery products (*5*). Because of the restricted sample sizes, however, it is not possible to apply this method in a nondestructive fashion to entire (packaged) foods. One option to overcome this is bigger diameter low-field NMR setups, which are typically used for magnetic resonance imaging (MRI). However, MRI machines are expensive, heavy, and sensitive pieces of equipment, which excludes routine application in most quality control or food verification applications. Nevertheless, some applications such as that have been suggested (*6*). An option that comes along at a much lower price and with a proven potential even for mobile use is single-sided NMR.

Single-sided—or inside-out—NMR sensors such as well-logging spectrometers (*7*) and the NMR-MOUSE (*8*) have been used for applications in the oil and polymer industries, respectively, for quite some time. The target materials for the NMR are relatively slow-diffusing in these applications. The same holds true for food materials with a high-fat content such as salmon tissue (*9*) or oil-in-water emulsions (*10*). Studies of materials with higher self-diffusion coefficients are hampered by large magnetic field gradients (about 10 T/m or even higher), which are typical for most single-sided NMR setups. In the presence of a magnetic field gradient, excited NMR magnetization experiences a decay not only due to transverse relaxation but also due to the diffusive displacement of the excited spins relative to the magnetic field gradient. This diffusion effect has been known since the early days of NMR (*11*) and leads to an effective transverse relaxation time $T_{2,\mathrm{eff}}$ (*9*), which is dependent on the echo time t_e:

$$\frac{1}{T_{2,\mathrm{eff}}} = \frac{1}{T_2} + \frac{1}{12}\gamma^2 G^2 D t_e^{\,2}$$

with T_2 denoting the "real" transverse relaxation time, γ denoting the gyromagnetic ratio of the excited nuclei, G denoting the strength of the magnetic field gradient, and D denoting the self-diffusion coefficient or the liquid phase. Even for relatively short echo times on the order of a few 100 μs, this echo attenuation will dominate over the one due to transverse relaxation and thus signals from fast-diffusing components will at least exhibit

* To whom correspondence should be addressed. Tel: ++49 6151 16 2934. Fax: ++49 6151 16 2833. E-mail: nikolaus.nestle@physik.tu-darmstadt.de.

10.1021/jf060431m CCC: $33.50
Published on Web 06/29/2006

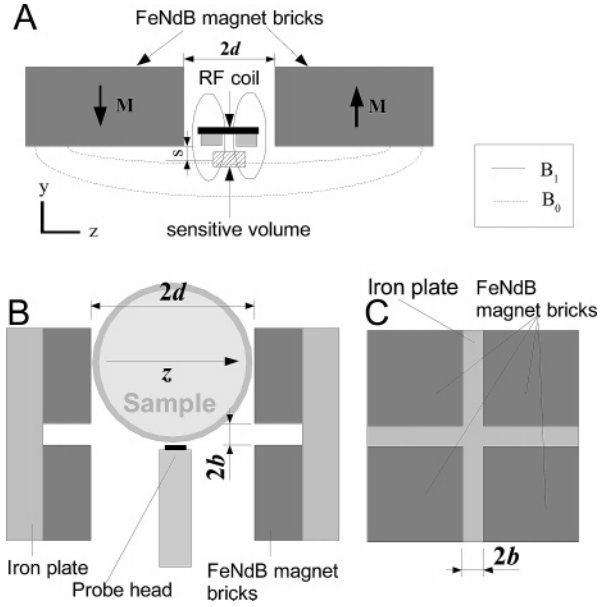

Figure 1. Magnet setups for (**A**) single-sided and semisingle-sided NMR. The semisingle-sided NMR setup (**B**) consists of a Helmholtz configuration (side view) of iron plates tiled with an array of four permanent magnet bricks (**C**, front view).

grossly distorted transverse relaxation rates (*9*, *10*) or even be attenuated so strongly that reasonable measurements are not possible at all any more. For spin−lattice relaxation time measurements, a strong background gradient mainly leads to a smaller sensitive volume and thus to a lower signal/noise ratio but not to a severe distortion as in the transverse relaxation times. (However, one also has to be aware that the higher fields typical for high-gradient single-sided magnet designs may compensate the smaller sensitive volume by higher sensitivity.) The fact that lower field strength is a price to be paid for more homogeneous field conditions in single-sided magnets is also known from some homogenized magnet designs in the literature (*12*, *13*).

In this contribution, two different approaches for a "single-sided" NMR sensor with a reduced magnetic field gradient will be described and the application of both sensors to unopened bottles of oxygen-supersaturated table water will be demonstrated. This takes up a suggestion made in an earlier publication on superoxygenated water (*14*). While there have been several publications on high-field NMR spectrocopy (in imaging magnets) on entire wine bottles recently (*15*, *16*), we are not aware of applications of low-field NMR to unopened bottles of beverages. In ref *16*, the carbon dioxide content of sparkling wine was measured.

MATERIALS AND METHODS

NMR Setups. Three different home-built low-field NMR setups were used for the experiments. (i) A conventional volume NMR setup (used as a reference system for the other setups) with an enclosing sample coil (26 windings of 1 mm isolated copper wire, 32 mm in diameter, 55 mm length) in a magnetic field produced by a Helmholtz-like configuration of two FeNdB permanent magnet disks (100 mm diameter, 18 mm height, obtained from Ningbo Ninggang Permanent Magnetic Materials Ldt., Ningbo, People's Republic of China) was used.

(ii) A single-sided NMR setup constructed from two FeNdB permanent magnet bricks (50.8 × 50.8 × 25.4 mm^3, obtained from Supermagnete-Webcraft GmbH, Uster, Switzerland) arranged in the way sketched in **Figure 1A** was used. By varying the distance between the two magnets, it was possible to obtain "homogenized" field regions with a gradient of about 1 T/m at distances of several millimeters from the magnets (further details and photos of the magnet setup are given in the Supporting Information). Further attempts to increase the homogeneity of the magnet by additional shimming of the magnets as they were also used for another homogenized single-sided NMR magnet (*17*) proved to be beneficial only in theory. With our magnets, the inhomogeneity due to the nonuniform magnetization inside the permanent magnets proved to dominate over the benefits from the shimming. The RF coil was elliptically shaped (15 mm × 40 mm) to match the geometry of the region of the homogeneous magnetic field. It was constructed from 20 turns of a flat copper band with about 2 mm width and 0.1 mm thickness and an insulation made from adhesive polymer tape. The inductivity of the coil was 13 μH, and its ohmic resistance was 1.1 Ω. The distance 2*d* between the two magnets was chosen as 46.8 mm in the experiment as a result of optimal sensitivity conditions for water in standard plastic bottles. In this case, the center of the sensitive volume was just inside the bottle (i.e., about 2 mm off the sensor surface).

Table 1. Properties of the Different NMR Setups Used in This Work

	(i) reference setup	(ii) single-sided	(iii) semisingle-sided
magnetic field strength (T)	0.127	0.122	0.136
proton resonance frequency, f_0 (MHz)	5.4	5.2	5.8
residual gradient (T/m) (determined by spin–echo)	<0.2	1	0.4
air gap (cm)	9		9
maximal sample volume (mL)	60	entire bottle	entire bottle
excited sample volume (mL)	ca. 30	<1	several
magnet system weight (kg)	4.5	3	12
approximate cost for permanent magnets (Euro)	300	80	320
signal/noise ratio in single shot on fully relaxed water sample	65	2.4	7.4
duration of RF pulse (90°) (μs)	2.7	3	3
typical time for determining a T1 of about 2 s (min)	2	45	10

(iii) A semisingle-sided NMR setup with a large gap, magnet system consisting of a Helmholtz-like configuration of two iron plates on which magnet bricks of the type that were also used in the single-sided magnet design were arranged in the way shown in **Figure 1B**,**C**. Photos of the setup are given in **Figure S3** of the Supporting Information. The distance between the two arrays of magnet bricks was chosen in a way that 1.5 L bottles fit in the gap of the magnet system (see the next section). For the spin−lattice relaxation measurements on oxygen-saturated water, the field homogeneity of the device was sufficient. Simulations indicate that smaller gradients can be achieved when optimizing the air gap and the distance between the magnets on each side according to the size of the magnet bricks (see **Figure S5** of the Supporting Information). For the measurements on entire bottles, the same probehead with a surface coil that was also used with the single-sided magnet configuration was placed inside the magnet in the way shown in **Figure 1B**. Like that, the sample finds itself in a relatively homogeneous magnetic field and the surface coil can excite a much bigger part of the sample volume than in the single-sided apparatus where the resonance conditions are only fulfilled in the "sweet spot". This probehead was used to keep the conditions comparable. Bigger RF coils would allow further gains in sensitivity.

Further details of the magnet systems can be found in **Table 1** and in the Supporting Information. The magnetic field simulations represented there were performed using EM studio (CST, Darmstadt, Germany).

The magnetic field strengths of the three setups are not completely matched (the semisingle-sided setup was constructed to achieve the maximal magnetic field with an air gap to accommodate entire bottles). However, as the frequency dependence of the oxygen relaxivity in water is only minor in the frequency range from 5 to 10 1/MHz (*18*, *19*), the variations in the oxygen relaxivity $r_{1,ox}$ between the different spectrometers can be neglected ($1/r_{1,Ox}\ dr_{1,Ox}/df_0 < 0.02$ MHz).

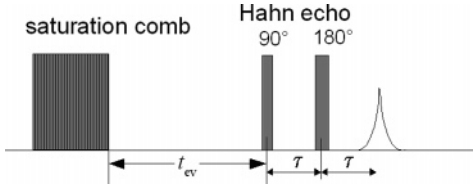

Figure 2. Echo-detected saturation recovery sequence for measuring longitudinal relaxation times in the presence of strong magnetic field gradients. In our experiments, we worked with a saturation comb consisting of five 90° pulses and with a fixed echo time 2τ of 300–500 μs. Phase cycling was not used.

The rather low field strength used in our setups was chosen as a compromise in order to keep the weight and cost of the magnet systems as low as possible (only standard commercial FeNdB brick or disk magnets were used; the maximal sizes of these magnets are limited as a result of transport safety legislation).

Calibration Procedures and Samples. For the NMR determination of dissolved oxygen in table waters, the longitudinal relaxation time of the water was measured. It was related to the oxygen concentration c_{Ox} according to the following relationship:

$$\frac{1}{T_1} = \frac{1}{T_{1o}} + r_{1,Ox}c_{Ox} \quad (1)$$

with T_{1o} denoting the relaxation time of the oxygen-free water.

As the relaxivity $r_{1,ox}$ of oxygen in water is field-dependent (*18*, *19*) and no sufficiently precise relaxation data at a proton resonance frequencies of 5−6 MHz are available in the literature, it was necessary to perform calibration measurements against samples with a known (supersaturated) oxygen concentration. As pointed out in ref *14*, the conventional methods for oxygen determination were not directly applicable to supersaturated oxygen concentrations. Therefore, we used a similar probe and dilute approach with subsequent electrochemical determination of the oxygen concentration as described in ref *14*. For electrochemical oxygen determination, a CellOx 325 sensor from WTW (Weilheim, Germany) was used. As the time required for measuring a relaxation time in the single-sided setup is much longer than in a volume setup, outgassing during the measurements proved to be a much graver problem. To avoid outgassing a set of 1.5 L polyethylene bottles with well-defined oxygen, partial pressure in the gas over the water was produced for testing the relaxivity calibration in the single-sided and semisingle-sided setup. The oxygen concentration in the bottles was determined from electrochemical measurements on 5−40 mL water samples at least 1 day after the preparation of the calibration bottles.

In the volume setup, the samples were filled in disposable 60 mL Luer−Lock syringes (Beckton-Dickinson, Meylan, France), which were kept under defined pressure during the measurement. Before the measurement, the pressurized syringes were allowed to equilibrate to ensure reproducible conditions in the syringe. After the NMR relaxometry experiments, the oxygen concentration in the water from the calibration bottles was again measured by the electrochemical sensor. For samples with an expected oxygen concentration of more than 30 mg/L, the dilution technique was used. Samples with lower concentration were measured directly. Calibration series were run for demineralized water and using water samples from two German brands of commercial oxygen-supersaturated table waters (Oxivit and active O_2). After calibration, measurements on commercial oxygen-supersaturated table waters in unopened stage and after opening were preformed. Some further relaxation time measurements were conducted on unopened bottles of wines and fruit wines, which were obtained from local supermarkets.

Pulse Sequences and Data Processing. Longitudinal relaxation time measurements were conducted using the echo-detected saturation−recovery (SR) sequence sketched in **Figure 2**. Transverse magnetization decay curves were recorded using a simple Hahn echo sequence (in order to quantify the magnetic field gradient effect in the different magnet systems).

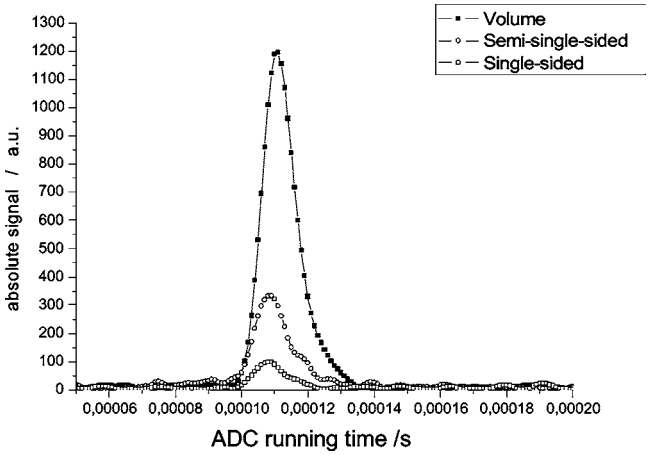

Figure 3. Signal intensity for the volume, semisingle-sided, and single-sided NMR systems for an oxygen concentration of 3 mg/L in commercial drinking water with brand name Oxivit and an evolution time of 6 s. Ten volume measurements, 25 semisingle-sided, and 46 single-sided measurements accumulations were used. The data were normalized for comparison of signals obtained with different numbers of accumulations.

In measurement series with signal intensities in the order of the noise level, the number of accumulations n for the different evolution times t_{ev} was adapted to achieve a uniform signal/noise ratio of the accumulated signal S/N for all evolution times. For monoexponential relaxation (which is the case in studies of dissolved oxygen or other paramagnetic species in a watery solvent) and a noise level that is independent of the signal amplitude, we can assume that

$$S/N \propto \sqrt{n}(1 - e^{-t_{ev}/T_1})$$

In this case, a uniform S/N can be achieved when choosing the number of signal accumulations

$$n \propto \left(\frac{1}{1 - e^{-t_{ev}/T_1}}\right)^2$$

In addition to the signal-independent noise level, there is also amplitude-dependent noise in a typical NMR signal. Therefore, a second term m is phenomenologically introduced in order to account for this noise contribution, too.

$$n = m + n_0 \cdot \left(\frac{1}{1 - e^{-t_{ev}/T_1}}\right)^2$$

The NMR experiments were controlled by a home-written two-layered NMR control software in which spectrometer driver core (open source development in C++ based at the institute, *20*) is run from a LabView (NI, Austin, TX) front end, which also performs the on-the-fly signal evaluation needed for the adaptive numbers of accumulations just described.

RESULTS AND DISCUSSION

Signal Quality and Characterization of the Different Magnet Systems. On all NMR systems, measurements were run to quantify the sensitivity and to characterize the field homogeneity of the magnet. To compare the sensitivity, the signal intensities recorded in an SR NMR experiment using the pulse sequence described in the third section of the Materials and Methods with an evolution time of 6 s were determined for a water sample with an oxygen content of 3 mg/L in all three setups. The results can be seen from **Figure 3**.

Calibration and Test Series in the Volume Magnet. The determination of the relaxivity was performed in the conventional volume NMR setup where also the signal intensity was best. The resulting calibration curve is shown in **Figure 4**.

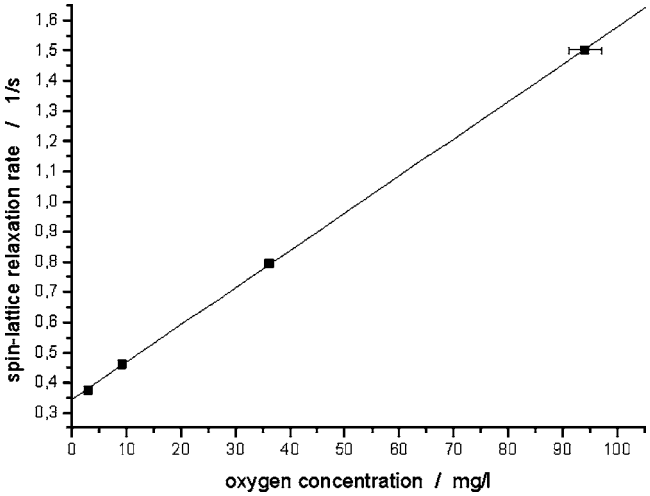

Figure 4. Determination of the oxygen relaxivity at 18 ± 1 °C and 5.4 MHz (in deionized water). From the slope of the calibration curve, we find a relaxivity $r_{1,Ox} = (122 \pm 2) \times 10^{-4}$ s^{-1} mg^{-1} L and a relaxation rate $R_0 = 1/T_{1o} = 0.348 \pm 0.005$ s^{-1} for the oxygen-free water.

The determined R_0 is in good agreement with ref *21*. The value determined for $r_{1,Ox}$ fits well with the values for other temperature and field conditions reported in the literature (*14*, *18*, *19*). The calibration was further checked by measurements of oxygenated water samples harvested from different bottles of commercial table waters. The results are presented in the Supporting Information (**Figure S6**). For both waters, the measured oxygen concentrations and relaxation times were in good agreement with the calibration values determinated from deionized water.

Measurements in the Single-Sided and Semisingle-Sided Setup. Figure 5 show the results obtained for a series of test bottles (prepared from Oxyvit, oxygen content stabilized by pressurization) in the single-sided and in the semisingle-sided NMR setup, respectively. As can be seen from the graphs, the measured relaxation times in both cases correspond very well to the calibration curve obtained in the volume setup. The measurements for both curves were conducted in a way that a similar signal/noise ratio was obtained. The measuring times to achieve this in the single-sided setup were about a factor of 4 longer than in the semisingle-sided setup (see also **Table 1**).

In **Figure 6**, semisingle-sided NMR measurements on a bottle of a commercial sample of oxygen-supersaturated water (Oxyvit) are given before and after opening of the bottle and taking water samples. The oxygen concentration observed in the first data points before opening of the bottle is about 10 mg/L higher than that observed immediately after opening the bottle. Relaxation time measurements were performed every 22 min. The time constant for the outgassing process was found to be 350 ± 55 min, and the residual oxygen concentration at the end of the outgassing process was extrapolated to 5.4 ± 1.6 mg/L, which is slightly lower than the value expected on the solubility of oxygen in water at atmospheric pressure (8.68 mg/L at 21 °C). The oxygen concentration in the bottle right after opening is 42 ± 3 mg/L according to the fit. This means that over 10% of the dissolved oxygen is lost very fast after opening the bottle. The time constant for the outgassing process is in good agreement with the observations for oxygenated water in plastic containers reported in ref *14*. The oxygen loss upon opening the bottles could not be measured in these experiments as the sampling of the oxygenated water was invasive.

Measurements on Wine Bottles. Dissolved oxygen is not the only possible solute that may lead to increased longitudinal

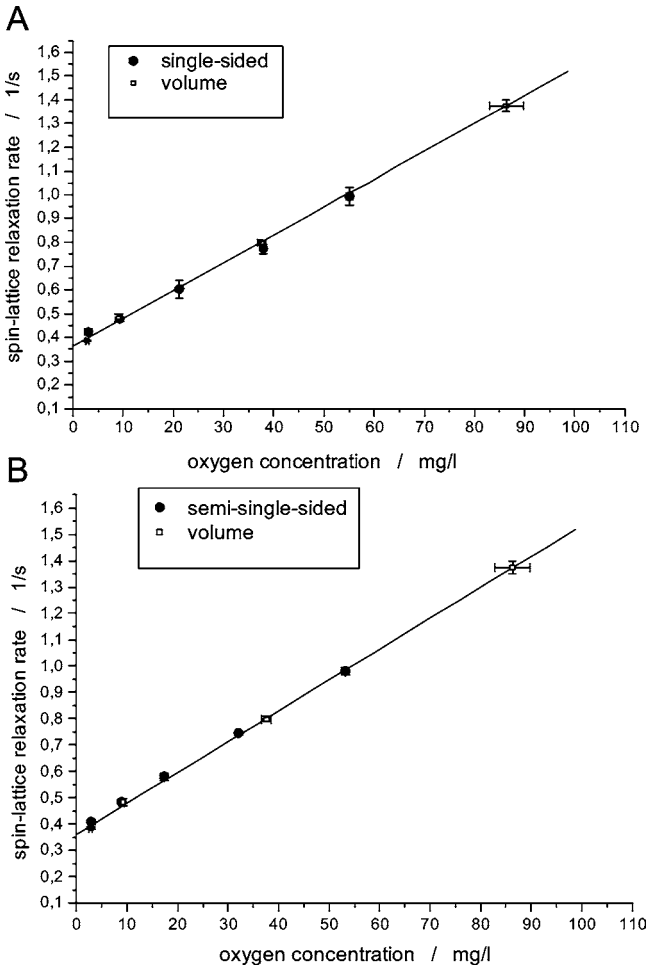

Figure 5. Spin–lattice relaxation rate measured with the single-sided and the semisingle-sided NMR sensor as compared with the results obtained in the volume NMR setup for different oxygen concentrations. The temperature was 18 ± 1 °C. To achieve a better signal/noise ratio, the measuring times for each relaxation time in these curves were several hours per data point in the single-sided setup and about 40 min in the semisingle-sided setup.

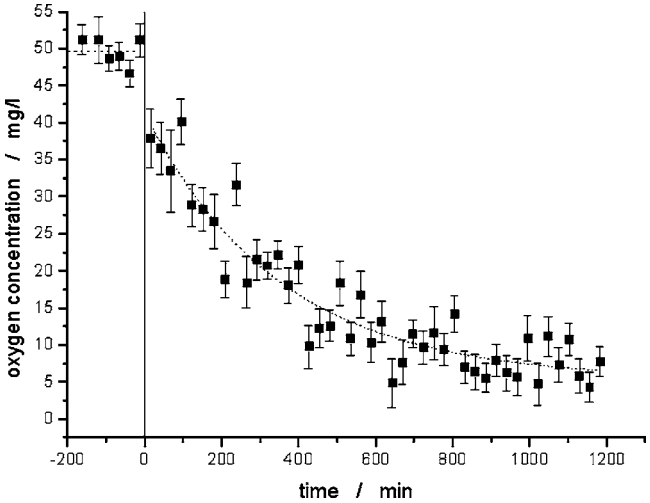

Figure 6. Oxygen concentration measurements by semisingle-sided NMR on a bottle of commercial oxygenated table water Oxyvit. Left of the line, before opening; right of the line, after opening.

relaxation rates in beverages: Dissolved paramagnetic metal ions also lead to a reduction of T_1. In drinking waters, sufficiently high concentrations (i.e., several mg l^{-1} of moder-

Table 2. Spin–Lattice Relaxation Times of Some Wines, Measured with the Semisingle-Sided NMR Setup at the Closed Bottle

	T_1 (s)
blueberry wine from Weinhof Reinheim (Reinheim, Germany)	0.199 ± 0.002
white wine, Pfefferer, from Schreckbichl (Girlan/South Tyrol)	1.16 ± 0.02
red wine, Rioja Crianza, from Ontañon (Quel, Spain)	1.19 ± 0.03

ately relaxing ions such as Cu^{2+} or about 1 mg L^{-1} of highly relaxing ions such as Fe^{3+} or Mn^{2+}) to seriously affect the relaxation times can be excluded both for health regulations and for taste reasons (except in some highly mineralized waters used for therapeutic purposes) (*14*, *22*). This is different in some fruit juices and wines. For example, pineapple or blueberry juice and some tea extracts are known to exhibit very short relaxation times (mainly due to Mn bound by organic complexing agents). Because of their short relaxation times, there even have been several studies about using such juices or extracts as contrast agents for MRI (*23*−*25*). NMR relaxometry on unopened bottles might become a valuable tool for studies of such beverages as well. As a proof of principle, we have performed relaxation time measurements on several bottles of ordinary (grape) wine and blueberry wine. The results are shown in **Table 2**.

As compared to blueberry juices and wines, which may contain up to 90 mg/L Mn (*26*), (grape) wine typically contains 1−2 mg/L Mn. However, in some red wines, values of up to 7.8 mg/L Mn have been reported (*27*). Under certain circumstances, NMR relaxometry on whole wine bottles may actually provide a nondestructive tool to verify claims of origin for certain vines known to exhibit high Mn concentrations. In any case, the NMR relaxometry method should be applicable for nondestructive distinction between products made from cultured blueberry and wild blueberry for which huge differences in the Mn content are reported (*26*).

DISCUSSION AND OUTLOOK

Our results demonstrate that single-sided NMR can be used for noninvasive measurements on foodstuffs with high self-diffusion coefficients such as beverages in closed bottles. While being the most lightweight and flexible setup, the single-sided NMR comes with two main disadvantages: sensitivity and the location of the sensitive volume quite close to the sensor surface. Both are intrinsic problems in single-sided NMR. Because of the relatively long T_1 values, the sensitivity problem is more severe in application to beverages than in previously published applications to polymers or fatty materials. The location of the sensitive volume prevented us from successful relaxometry experiments on beverages in glass bottles with the single-sided setup.

As bottled beverages and also most other samples in food science do not come in arbitrarily big sizes, a semisingle-sided sensor allows all of the flexibility needed with respect to the sample size and at the same time offers several advantages with respect to sensitivity, intrusion depth, and a smaller background gradient. This type of sensor therefore seems to be the most appropriate tool for nondestructive NMR relaxation measurements not just in beverages but also in many other food science applications. The required magnet system can be constructed from widely available, low-cost, permanent magnet bricks.

Further improvements in this type of NMR sensor can be expected from the design of semiflexible, larger surface coils (as they are common in medical applications, see *28*), which allow an even better filling factor than in our demonstration experiments. Such coils and a magnet housing with thermal insulation (and possibly temperature stabilization) are the next steps to go in developing the semisingle-sided NMR relaxation sensors into a tool for practical applications in food science.

ACKNOWLEDGMENT

We are grateful to CST for providing us a free license for EM-studio and to Tom Schiedek (TUD, Institut für Angewandte Geowissenschaften) for lending us the CellOx 325 electrochemical oxygen sensor.

Supporting Information Available: Photographs of probe heads and magnet systems, field simulations, and measured magnetic fields for the single-sided and semisingle-sided magnet system, comparison of calibration curve, and measurements on different types of table waters. This material is available free of charge via the Internet at http://pubs.acs.org.

LITERATURE CITED

(1) Samuelsson, E. G.; Vikelsoe, J. Estimation of the amount of liquidfat in cream and butter by low resolution NMR. *Milchwissenschaft* **1971**, *26*, 621−625.

(2) Lambelet, P. Comparison of NMR and DSC methods for determining solid content of fats. Application to cocoa butter and its admixtures with milk fat. *Lebensm.-Wiss. Technol.* **1983**, *16*, 200−202.

(3) Le Dean, A.; Mariette, F.; Le Marin, M. ^{1}H nuclear magnetic resonance relaxometry study of water state in milk protein mixtures. *J. Agric. Food Chem.* **2004**, *52*, 544−5455.

(4) Chatakanonda, P.; Dickinson, L. C.; Chinachoti, P. Mobility and distribution of water in cassava and potato starches by ^{1}H and ^{2}H NMR. *Agric. Food Chem.* **2003**, *51*, 7445−7449.

(5) Engelsen S. B.; Jensen, M. K.; Pedersen, H. T.; Nørgaard, L.; Munck, L. NMR-baking and multivariate prediction of instrumental texture parameters in bread. *J. Cereal Sci.* **2001**, *33*, 59−69.

(6) Saito, K.; Miki, T.; Hayashi, S.; Kajikawa, H.; Shimada, M.; Kawate, Y.; Nishizawa, T.; Ikegaya, D.; Kimura, N.; Takabatake, K.; Sugiura, N.; Suzuki, M. Application of magnetic resonance imaging to nondestructive void detection in watermelon. *Cryogenics* **1996**, *36*, 1027−1031.

(7) Kleinberg, R. L. Well logging. In *Encyclopedia of Nuclear Magnetic Resonance*; Grant, D. M., Harris, R. K., Eds.; Wiley: Chichester, United Kingdom, 1996; Vol. 8, pp 4960−4969.

(8) Guthausen, A.; Zimmer, G.; Blümler, P.; Blümch, B. Analysis of polymer materials by surface NMR via the MOUSE. *J. Magn. Reson.* **1998**, *130*, 1−7.

(9) Veliyulin, E.; van der Zwaag, C.; Burk, W.; Erikson, U. In vivo determination of fat content in Atlantic salmon (Salmo salar) with a mobile NMR spectrometer. *J. Sci. Food Agric.* **2005**, *85*, 1299−1304.

(10) Pedersen, H. T.; Ablett, S.; Martin, D. R.; Mallett, M. J. D.; Engelsen, S. B. Application of the NMR-MOUSE to food emulsions. *J. Magn. Reson.* **2003**, *165*, 49−58.

(11) Hahn, E. Spin−echoes. *Phys. Rev.* **1950**, *80*, 580−594.

(12) Fukushima, E.; Jackson, J. A. Unilateral magnet having a remote uniform field region for nuclear magnetic resonance. U.S. Patent 6,489,872, 1999.

(13) Marble, A. E.; Mastikhin, I. V.; Colpitts, B. G.; Balcom, B. J. An analytical methodology for magnetic field control in unilateral NMR. *J. Magn. Reson.* **2005**, *174*, 78−87.

(14) Nestle, N.; Baumann, T.; Niessner, R. Oxygen determination in oxygen-supersaturated drinking waters by NMR relaxometry. *Water Res.* **2003**, *37*, 3361−3366.

(15) Weekley, A. J.; Bruins, P.; Sisto, M.; Augustine, M. P. Using NMR to study full intact wine bottles. *J. Magn. Reson.* **2003**, *161*, 91−98.
(16) Autret, G.; Liger-Belair, G.; Nuzillard, J. M.; Parmentier, M.; Dubois de Montreynaud, A.; Jeandet, P.; Doan, B. T.; Beloeil, J. C. Use of magnetic resonance spectroscopy for the investigation of the CO2 dissolved in champagne and sparkling wines: A nondestructive and unintrusive method. *Anal. Chim. Acta* **2005**, *535*, 73−78.
(17) Perlo, J.; Demas, V.; Casanova, F.; Meriles, C. A.; Reimer, J.; Pines, A.; Blümich, B. High-resolution NMR spectroscopy with a portable single-sided sensor. *Science* **2005**, *308*, 1279.
(18) Hausser, R.; Noack, F. Nuclear spin relaxation and correlation in the system water-oxygen (original in German: Kernmagnetische relaxation und korrelation im system wasser-sauerstoff). *Z. Naturforsch.* **1965**, *20a*, 1668−1675.
(19) Teng, C. L.; Hong, H.; Kühne, S.; Bryant, R. G. Molecular oxygen spin−lattice relaxation in solutions measured by proton magnetic relaxation dispersion. *J. Magn. Reson.* **2001**, *148*, 31−34.
(20) Gädke, A.; Schmidt, C.; Stork, H.; Nestle, N. A flexible hardware and software platform for low-cost (mobile) NMR systems XIII AMPERE NMR Summer School, Zakopane, Poland, 5.-10.6.2005.
(21) Simpson, J. H.; Carr, H. Y. Diffusion and nuclear spin relaxation in water. *Phys. Rev.* **1958**, *111*, 1201−1202.
(22) For example, German drinking water regulations. TrinkwV: dissolved Fe, <0.2 mg/L; dissolved Mn, <0.05 mg/L; and dissolved Cu, <3 mg/L.
(23) Hiraishi, K.; Narabayashi, I.; Fujita, O.; Yamamoto, K.; Sagami, A.; Hisada, Y.; Saika, Y.; Adachi, I.; Hasegawa, H. Blueberry juice: Preliminary evaluation as an oral contrast agent in gastrointestinal MR imaging. *Radiology* **1995**, *194*, 119−123.
(24) Riordan, R. D.; Khonsari, M.; Jeffries, J.; Maskell, G. F.; Cook, P. G. Pineapple juice as a negative oral contrast agent in magnetic resonance cholangiopancreatography: A preliminary evaluation. *Br. J. Radiol.* **2004**, *77*, 991−999.
(25) Mino, Y.; Yamada, K.; Takeda, T.; Nagasawa, O. Metal-containing components in medicinal plants. III. Manganese-containing components in Theae folium as oral magnetic resonance imaging contrast materials. *Biol. Pharm. Bull.* **1996**, *44*, 2305−2308.
(26) Wallrauch, S.; Greiner, G. Zur Unterscheidung von Erzeugnissen aus Wild- und Kulturheidelbeeren. *Flüssiges Obst.* **2005** (1/2005), 14−17.
(27) Cabrera-Vique, C.; Teissedre, P. L.; Cabanis, M. T.; Cabanis, J. C. Manganese determination in grapes and wines from different regions of France. *Am. J. Enol. Vitic.* **2000**, *51*, 103−107.
(28) Vlaardingerbroek, M. T.; den Boer, J. A. *Magnetic Resonance Imaging. Theory and Practice*; Springer: Heidelberg, 1999.

Received for review February 13, 2006. Revised manuscript received May 20, 2006. Accepted May 31, 2006. This work was funded by the German ministry of research and the state of Hesse as a part of the installation of the first Juniorprofessuren.

JF060431M